SCIENTIFIC PAPERS
OF THE UNIVERSITY OF PARDUBICE
Series A
Faculty of Chemical Technology
3 (1997)

VOLTAMMETRIC DETERMINATION OF TITANIUM, VANADIUM, AND MOLYBDENUM USING A CARBON PASTE ELECTRODE MODIFIED WITH CETYLTRIMETHYLAMMONIUM BROMIDE

Monika STADLOBER, Kurt KALCHER[1] and Georg RABER
Institute of Analytical Chemistry, Karl-Franzens University,
A-8010 Graz

Received September 12, 1997

Methods for the voltammetric determination of titanium, vanadium, and molybdenum using a carbon paste electrode modified in situ with cetyltrimethylammonium bromide (CTAB) are described. Titanium and vanadium are preconcentrated at the electrode surface via their anionic oxalate complexes from acidic solution at -1.2 and -0.9 V vs. the saturated calomel electrode. The accumulation process is due to in situ formation of an ion-exchanger at the electrode surface by adsorption of the surfactant, and to formation of ion-pairs or micellar congregates, since the concentration of CTAB is higher than the critical micellar concentration (CMC). Simultaneously during accumulation, titanium(IV)- and vanadium(V)-oxalates are reduced to their tri- and tetravalent states. The preconcentration of molybdenum(VI) was performed by adsorption and of ion-pairs of cetyltrimethylammonium and Mo(VI)-oxalates at a potential of -0.4 V. Molybdenum(VI)-oxalate is reduced to a mixed-valence compound of

---

[1] To whom correspondence should be addressed.

Mo(VI) and (V). Linear dependence of current on concentration exists in the ranges of 10 to 250 $\mu g\ l^{-1}$ for titanium, 5 to 200 $\mu g\ l^{-1}$ for vanadium, and 5 to 500 $\mu g l^{-1}$ for molybdenum, when applying a preconcentration time of 1 min. The limit of detection (calculated as 3σ) is 0.1 $\mu g\ l^{-1}$ Ti, 0.07 $\mu g\ l^{-1}$ V, and 0.04 $\mu g\ l^{-1}$ Mo with a deposition time of 10 min. The method presented in this report shows that CTAB is a suitable agent for modification of CPEs giving good reproducibility of results.

Introduction

Electrochemistry of titanium is limited to the one-electron reduction of Ti(IV) to Ti(III), or the reverse oxidation [1]. Lingane et al. described the redox behavior of titanium in strong mineral acids [2]. They found reversibility of the redox reaction only at high hydrogen ion concentrations. By complexing titanium(IV) with organic acids, such as oxalic acid, ethylenediaminetetraacetic acid (EDTA), citric acid, tartaric acid, salicylic acid, and mandelic acid, the electrode reaction becomes more reversible and can better be exploited for polarographic/voltammetric measurements [3-6].

The electrochemical behavior of vanadium and molybdenum is rather complex due to the large number of different species which exist in solution as well as to the various oxidation states, into which they can be transformed. Vanadate and molybdate show quite a high capability to undergo acid-base and polymerization reactions, where the species formed are strongly dependent on pH of the solution and the concentration of the analyte [7-10].

At mercury electrodes, the redox-couple vanadium(V)/(IV) cannot be studied easily in acidic media, because vanadium(V) reacts chemically with mercury, whereas the oxidation of vanadium(IV) does not occur within the attainable potential range. Therefore, the use of solid electrodes, such as platinum or pyrolytic graphite was recommended [11,12].

Mo(VI) cannot be reduced at the dropping mercury electrode in neutral or alkaline solutions without addition of complexing agents. In acidic media two to four reduction waves are observed, of which at least two can be assigned to the reduction to Mo(V) and further reduction to Mo(III) [10]. After introducing complexing agents, such as different carboxylic acids, two reduction waves are observed in most cases representing the reduction to the penta- and trivalent state [13].

For trace determinations of titanium, vanadium, and molybdenum adsorptive stripping voltammetric techniques were applied after converting titanium(IV), vanadium(V), or Mo(VI) into stable complexes with various organic ligands. Solochrome Violet RS, Cupferron, catechol, pyrogallol, Pyrocatechol Violet, Beryllon III, or 4-(2-pyridylazo)-resorcinol are excellent complexing agents for titanium or vanadium [14-20]. Molybdenum forms stable complexes with 8-hydroxyquinoline, Eriochrome Blue Black R, or phenanthroline - fulvic acid, which adsorb onto the mercury electrode [21-23]. With phosphate molybdenum also forms the well adsorbable 12-molybdo-phosphate [24,25].

Another possibility to improve the detection limit is the exploitation of catalytic effects of some reagents on the redox-reactions of the elements under investigation. Transition metals in lower oxidation states are known to be oxidized by agents such as hydrogen peroxide, bromate, chlorate, perchlorate, or nitrate. Thus, the presence of such reactants increases the reduction current by chemical oxidation of the reduced species, producing the catalytic effect. The best performance, however, was achieved by combination of adsorptive stripping voltammetry with electrocatalysis [26-35].

Carbon paste electrodes (CPEs) have attracted considerable attention during the past two decades due to their ease of handling and modification [36,37]. So far, no studies on the electrochemical determination of titanium with the use of carbon paste electrodes (CPEs) have been published. Up to now, only one method has been described in the literature, where small concentrations of vanadium are determined in solution by CPEs [38]. CPEs were also rarely used for the determination of molybdenum traces. Monien et al. [39,40] exploited the adsorption of molybdenum as a complex with diethyldithiocarbamate onto a CPE under open circuit conditions.

In the present work our interest is focused on the applicability of carbon paste electrodes for the determination of trace concentrations of titanium, vanadium, and molybdenum.

Within our investigations on the modification of CPEs we found that cetyltrimethylammonium bromide (CTAB) is able to preconcentrate titanium, vanadium, and molybdenum as their anionic oxalate complexes at the electrode surface, and can subsequently be stripped anodically [41-43]. This paper describes sensitive voltammetric methods for the determination of titanium(IV), vanadium(V), and molybdenum(VI) with CPEs by an adsorptive modification of the electrode with CTAB and accumulation of the transition elements as oxalate complexes

Experimental

Apparatus

The voltammetric experiments were performed with a voltammetric analyzer (model 264A PAR, Princeton Applied Research) in combination with an automatically controlled self-constructed cell compartment made of Plexiglas [44]. The cell consisted of a titration vessel of glass (20–60 ml; 6.1415.220, Metrohm) with a platinum wire as counter electrode and a saturated calomel electrode (SCE, 303-NS, Ingold) as reference. The latter was in contact with the solution *via* a salt bridge (1 M KCl) with a Vycor frit to avoid contamination of the reference electrode. The solution in the cell could be stirred (ca. 300 rpm) with a PTFE coated stirring bar when required; it was deaerated with highly pure argon (99.999%) for at least 5 minutes prior to voltammetric measurements. During the measurements argon was passed over the solution. Deaeration is not necessary with respect to the voltammetric signals in the positive potential range, but decreases the background current in this region.

Voltammetric curves were registered either on a X–Y-recorder (Compensograph X–Y 1929, Siemens) or transferred to a personal computer after analogue to digital conversion by an appropriate interface [45].

Working Electrode

The body of the carbon paste electrode consisted of a PTFE rod (outer diameter 10 mm) with a 3 mm deep centric hole (diameter 7 mm) for the carbon paste filling and a platinum wire through the center of the rod for electric contact.

The carbon paste was prepared by thoroughly mixing five grams of spectral carbon powder (RWB, Ringsdorff-Werke, Germany) with 1.6 ml paraffin oil (Uvasol, Merck) until a homogeneous consistency was achieved. The paste was packed into the electrode and smoothed off with a PTFE plate.

Reagents

Deionized water was distilled twice in a quartz still and then purified by a cartridge deionization system (Nanopure, Barnstead). Oxalic acid and sodium acetate were of suprapure grade (Merck). All other chemicals were of analytical grade (p.a., Merck). Cetyltrimethylammonium bromide was recrystallized from a 4:1 (v/v) acetone-methanol mixture prior to use. Stock solutions of titanium (1000 mg l^{-1} Ti) were prepared by dissolving 0.6642 g potassium titanyl oxalate (Ventron, Karlsruhe, Germany) in 100 ml 0.1 M aqueous oxalic acid. Solutions of vanadium(V) (1000 mg l^{-1} V(V)) were prepared by dissolving 0.2394 g sodium vanadate (p.a., Merck) in 100 ml 0.3 M nitric acid. The molybdenum(VI) standard solution (1000 mg l^{-1} Mo(VI) as $(NH_4)_6Mo_7O_{24}\cdot 4H_2O$ in diluted ammonia solution) was purchased from Merck (Titrisol Merck Art. 9926). Stock solutions of lower concentrations were prepared freshly by dilution with water. Stock solutions of salts used for investigations on their interference had a concentration of 1 or 10 g l^{-1} with respect to the ion.

Procedure

Titanium

Voltammetry

The supporting electrolyte for the voltammetric measurements consisted of 0.05 M acetate-buffer and 0.01 M oxalic acid (pH 4.3). CTAB was added in a concentration of 10^{-4} mol l^{-1}.

Cyclic voltammograms (CVs) were recorded from −1.2 to 0 V with a scan rate of 20 mV s^{-1}m and an equilibration time of 30 seconds, beginning in anodic direction.

All quantitative measurements were performed in differential pulse mode (DPV). The initial potential was −1.2 V, the final 0 V, the pulse height 50 mV, and the scan rate 10 mV s^{-1}. Prior to the DPV-measurements the electrode was conditioned by applying a potential of −1.2 V for 15 minutes in the supporting electrolyte containing CTAB. Subsequently, titanium was added to the solution and preconcentrated onto the electrode surface with the initial potential applied.

Regeneration

Complete removal of residual titanium from the electrode was achieved by exposing the electrode to a separate solution containing 0.1 M sodium salicylate and 0.05 M acetate buffer (pH 4.7), applying a potential of −1.2 V for 1 min and scanning to -0.2 V. After this, the cleaning was completed by a 1 minute exposure of the electrode to a stirred solution of 1 M potassium bromide without application of potential.

Analysis of a Mineral Sample (Stone-wool) Heralan, HERAKLITH, Austria

About 200 mg of the sample were fused with a 5-fold excess of $NaKCO_3$ in a platinum crucible for 20 minutes. Afterwards the reaction product was dissolved in 50 ml of hydrochloric acid (5 M). The resulting solution containing solid silicate was heated on a sand bath until most of the hydrochloric acid was evaporated. Then again HCl (15 ml, 10 M) was added and evaporated almost to dryness. This procedure was repeated 2 times. The residue was dissolved in hydrochloric acid (3 M), and the silicic acid was filtered off. The filtrate was diluted up to a volume of 100 ml. For the voltammetric determination an aliquot of 10 µl was added to 20 ml of supporting electrolyte. For quantitative evaluations the internal standard addition method was used.

Vanadium

Voltammetry

The supporting electrolyte for the voltammetric measurements consisted of 0.01 M oxalic acid. CTAB was added in a concentration of 2.5×10^{-4} mol l^{-1}.

Cyclic voltammograms (CV) were recorded from −0.9 to +0.8 V with a scan rate of 20 mV s^{-1} and an equilibration time of 30 s, starting in anodic direction. The initial potential for DPVs was −0.9 V, the final +0.7 V, the pulse height 50 mV, and the scan rate 20 mV s^{-1}. Conditioning was performed by applying a potential of −0.9 V for 15 minutes in the supporting electrolyte containing CTAB.

Regeneration

The regeneration solution consisted of 0.1 M sodium salicylate and 0.005 M oxalic acid. The regeneration process was the same as with titanium.

Analysis of a Fuel Oil Sample

Approximately 0.5 g of the fuel oil was weighed in a porcelain crucible. The sample was warmed softly with a burner to ignition of the sample and continued to complete combustion. The residue was then calcinated at 600 °C for 2 to 3 hours. After cooling, 0.25 ml of a mixture of nitric and sulfuric acid (1:1) was added and diluted to 10 ml with water.

For the voltammetric determination aliquots of 30 or 50 μl were added to 20 ml of supporting electrolyte.

Molybdenum

Voltammetry

The supporting electrolyte for the voltammetric measurements consisted of 0.01 M oxalic acid. CTAB was added in a concentration of 7.5×10^{-5} mol l^{-1}.

Cyclic voltammograms (CV) were recorded either from −1.2 or from −0.4 to +0.8 V with a scan rate of 20 mV s^{-1}, starting in anodic direction after an equilibration time of 30 s with the initial potential applied.

DPVs were recorded with the initial potential of −0.4 V and the final potential of +0.7 V. The other conditions were the same as for vanadium.

Regeneration

Residual molybdenum species from the electrode surface were removed by exposing the electrode to a solution containing 0.005 M oxalic acid with a potential of -1.2 V applied for 1 min.

Analysis of a Steel Sample

Approximately 100 mg of the steel were weighed in a 100 ml glass vessel and 20 ml concentrated hydrochloric acid were added. The acid was heated on a burner until most of the hydrochloric acid had evaporated. This procedure was repeated 3 times. The residue was dissolved in 10 ml diluted HCl (3 %) and made up to a volume of 100 ml with water.

Results and Discussion

The titanyl cation TiO^{2+} forms a stable anionic complex with oxalic acid with a formation constant of 5×10^{10} $l^2\,mol^{-2}$ according to Eq. (1) [46]

$$TiO^{2+} + 2(C_2O_4)^{2-} \rightleftharpoons [TiO(C_2O_4)_2]^{2-} \tag{1}$$

At a mercury electrode reduction occurs at about -0.3 V vs. SCE at pH 1.2 (Eq. 2) [3]

$$TiO(C_2O_4)]^{2-} + 2H^+ + e^- \rightleftharpoons [Ti(C_2O_4)_2]^- + H_2O \tag{2}$$

When using a CPE, reduction of $[TiO(Ox)_2]^{2-}$ occurs at about -0.9 V (pH = 4.3) as a weak signal superimposed on the hydrogen evolution current. This can be seen clearly in the cyclic voltammogram recorded with an unmodified electrode (Fig. 1A).

The electrode reaction is rather irreversible, since reoxidation is anodically shifted to about -0.05 V. When lowering the pH the shift becomes less, but the signal still is irreversible. Since the signals are always very small, the sensitivity is low and not suitable for trace analysis.

If CTAB is present in the solution at a concentration level higher than CMC, the titanium oxalate becomes preconcentrable at the electrode surface and yields a pronounced reduction and reoxidation signal of the redox couple $[TiO(Ox)_2]^{2-}/[Ti(Ox)_2]^-$ with a tremendous improvement in sensitivity (Fig. 1B).

The redox reaction without CTAB is strongly irreversible, but it becomes quasi-reversible in its presence. The potentials of reduction and reoxidation lie at about -0.78 and -0.64 V vs. SCE, respectively. The reduction signal shifts to more positive potentials compared to unmodified carbon paste electrodes.

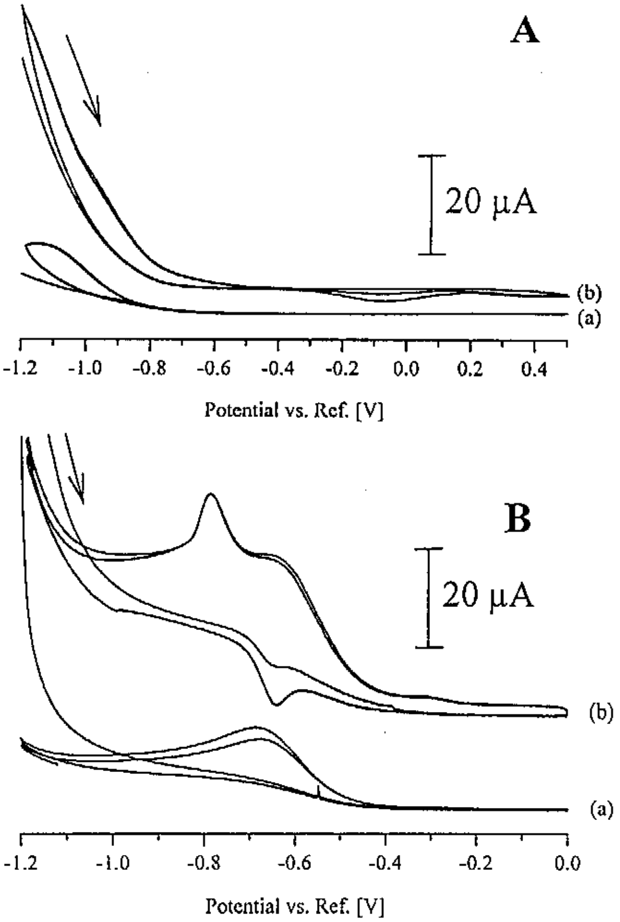

Fig. 1 Cyclic voltammograms of titanium(IV) at a plain (A) and a CTAB-modified (B) carbon paste electrodes; equilibration time 30 s, initial potential -1.2 V, final potential (A) +0.5 V, (B) 0 V, scan rate 20 $mV\,s^{-1}$. A: (a) 0, (b) 250 $mg\,l^{-1}$ titanium, supporting electrolyte 0.1 M KCl, 0.05 M acetate buffer, 0.01 M oxalic acid; B: (a) 0, (b) 0.5 $mg\,l^{-1}$ titanium; supporting electrolyte 0.05 M acetate buffer, 0.01 M oxalic acid, 0.1 mM CTAB

This indicates that Ti(IV) is more easily reduced in the adsorbed form with cetyltrimethylammonium ions (CTA^+) than as a free complex in solution. On the other hand, the reoxidation potential shifts to more negative values due to enhanced reversibility. Titanyl oxalate apparently shows a high affinity towards the positively charged CTA^+. Additionally it can be seen that the electrochemical response of titanium is overlapped by a broad wave caused by CTAB. The reduction peak appearing at around -0.7 V results from the reduction of oxygen containing groups at the electrode surface. It usually arises with unmodified electrodes at approx. -0.9 V and is shifted in anodic direction in the presence of the surfactant. It is independent of the presence of analyte in solution

Ion-pairing reagents other than CTAB, comprising lipophilic cations, such as tetrabutyl-ammonium bromide (TBAB), tetrabutylphosphonium bromide (TBPB), tetraphenyl-phosphonium chloride (TPPC), or tetraphenylarsonium chloride (TPAC) were found to have an improving, but only small effect on the determination of titanium. This is due to the fact that the hydrophobic part of the counter ion is attracted by the lipophilic carbon paste, forming a monomolecular layer at the electrode surface, but interacts only slightly with titanyl oxalate. However, under open circuit conditions preconcentration of titanyl oxalate in the presence of the cationic surfactants is not effective.

The highest peak currents and the most reproducible results are obtained with an *in situ* modification of the surface of the carbon paste electrode with CTAB.

Titanium as an oxalate complex can be preconcentrated onto the surface of CPEs in the presence of CTAB, if a deposition potential more negative than –0.7 V is applied. If CTAB is used as a modifier in a separate solution under open circuit conditions titanium is also preconcentrable, but only to a much smaller extent requiring significantly higher Ti concentrations, probably due to washing out of accumulated species by medium exchange. Thus, application of a preconcentration potential for the determination of titanium at lower concentrations is essential.

The accumulation process can be explained in analogy to reversed phase ion-pair partitioning chromatography by two effects, i.e. *in situ* formation of an ion-exchanger at the electrode surface (A), and formation of ion-pairs or micellar congregates in solution (B) (Eqs (3)–(6)).

(A)

$$[\mathrm{CTA}^+]_{x,mic.,sol.} \xrightarrow{-1.2\,\mathrm{V}} [\mathrm{CTA}^+]_{x,mic.,surf.} \tag{3}$$

$$[\mathrm{CTA}^+]_{x,mic.,surf.} + y\,[\mathrm{TiO(C_2O_4)_2}]^{2-}_{sol.} \longrightarrow \langle [\mathrm{CTA}^+]_x\{[\mathrm{TiO(C_2O_4)_2}]^{2-}\}_y\rangle_{surf.} \tag{4}$$

(B)

$$[\mathrm{CTA}^+]_{x,mic.,sol.} + y[\mathrm{TiO(C_2O_4)_2}]^{2-}_{sol.} \longrightarrow \left\langle [\mathrm{CTA}^+]_x\{[\mathrm{TiO(C_2O_4)_2}]^{2-}\}_y\right\rangle_{sol.} \tag{5}$$

$$\left\langle [\mathrm{CTA}^+]_x\left\{[\mathrm{TiO(C_2O_4)_2}]^{2-}\right\}_y\right\rangle_{sol.} \xrightarrow{-1.2\,\mathrm{V}} \left\langle [\mathrm{CTA}^+]_x\left\{[\mathrm{TiO(C_2O_4)_2}]^{2-}\right\}_y\right\rangle_{surf.} \qquad (6)$$

The indices *sol* and *surf* designate the bulk solution and the electrode surface, respectively; *mic* indicates micelle.

When the concentration of CTAB in solution is above CMC, mass transport and adsorption is probable via micelles rather than via individual surfactant ions [47]. At the CTA^+ concentrations below the critical micellar concentration only monomers are adsorbed on the electrode surface; therefore, the background current is low but the transport of the titanyl oxalate anions towards the electrode surface can be performed only with monomers, which is obviously not so effective.

The titanyl oxalate anion will be reduced simultaneously during the adsorption

$$\left\langle [\mathrm{CTA}^+]_x\left\{[\mathrm{TiO(C_2O_4)_2}]^{2-}\right\}_y\right\rangle_{surf.} + 2y\mathrm{H}^+ + y\mathrm{e}^- \xrightarrow{-1.2\,\mathrm{V}} \left\langle [\mathrm{CTA}^+]_x\left\{[\mathrm{Ti(C_2O_4)_2}]^{-}\right\}_y\right\rangle_{surf.} + y\mathrm{H_2O} \qquad (7)$$

When preconcentrating Ti in the presence of CTAB there is an overlap of the peak in the blank curve with the titanium signal. In principle, DPV could be recorded in both directions yielding a response for titanium, but scanning in anodic direction yields much higher peak currents, as negative deposition potentials have a favorable effect on the adsorption of CTA^+ micelles. Simultaneously, reduction of $[TiO(Ox)_2]^{2-}$ occurs yielding $[Ti(Ox)_2]^-$, which is ensuingly immobilized by ion-pairing. Therefore, the reoxidation signal, recorded in the anodic scan is much more pronounced than the corresponding reduction peak. Another reason for exploiting the reoxidation signal is that its height can be evaluated much better, because of lower background currents and only a very small overlapping signal of the blank curve. Anodic differential pulse voltammograms are shown in Fig. 2.

As expected the peak currents increase with increasing negative deposition potentials. The titanium reoxidation current increases linearly from −0.7 V to −1.3 V. The more negative the applied deposition potential, the more effective is adsorption of the positively charged CTA^+ micelles, and thus the better is the transport of titanyl oxalate to the electrode surface. For practical reasons a deposition potential of −1.2 V was found optimal.

Optimization of the CTAB-concentration in solution shows that only concentrations above the CMC are effective for preconcentrating titanium at low concentrations. The CMC for CTAB was determined by conductivity measure-

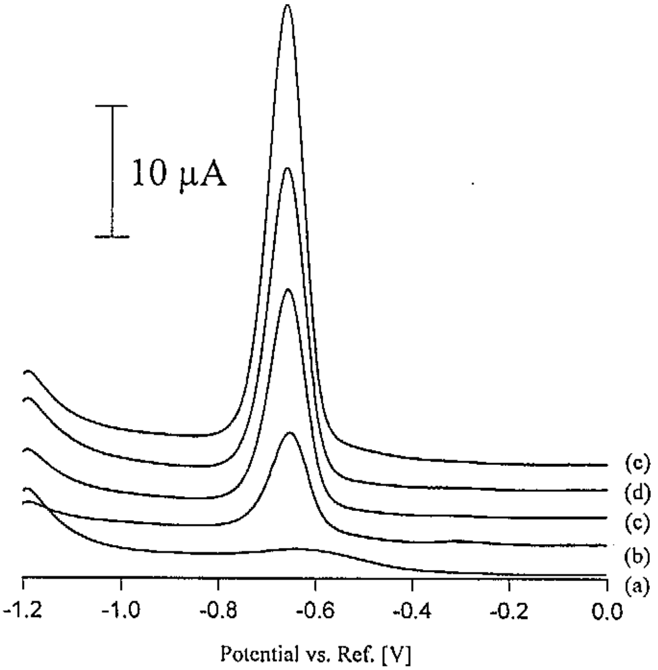

Fig. 2 Differential pulse voltammograms of Ti(IV) with a CPE modified *in situ* with CTAB; supporting electrolyte 0.05 M acetate buffer, 0.01 M oxalic acid, 0.1 mM CTAB; 2 min deposition at −1.2 V; Ti(IV) concentration (a) 0, (b) 30 μg l^{-1}, (c) 60 μg l^{-1}, (d) 90 μg l^{-1}, (e) 120 μg l^{-1}

ments and was found to be approximately 0.075 mM in the supporting electrolyte. The maximum titanium oxidation signals are obtained with a concentration of about 0.15 mM CTAB. When the CTAB concentration is increased further, the peak current decreases slowly, whereas the background current increases. Although peak currents have the maximum value at a concentration of 0.15 mM, the best results concerning reproducibility were obtained with only 0.1 mM CTAB.

Other parameters which influence the analytical performance of the determination of titanium to a great extent are the composition and the pH of the measurement solution. The best results were achieved with a solution containing acetate buffer (0.05 M) and oxalic acid (0.01 M) (pH 4.3).

When studying the influence of pH by addition of hydrochloric acid or sodium hydroxide to this solution, the optimum was found at a value of 4.3. At pH 7 no reoxidation could be observed anymore. This is also valid when decreasing the pH to 1.5. Also the peak potential depends on the hydrogen ion concentration and decreases linearly with decreasing H^+ concentration with a slope of about 100 mV per pH unit. This suggests that two hydrogen ions are involved in the redox process according to Eq. (2).

The complete removal of accumulated titanium from the CTA$^+$-modified electrode surface requires further treatment of the electrode for repeated use (regeneration). It was necessary to clean the electrode surface by electrochemical desorption of residual CTA$^+$-titanyl oxalate ion pairs. It was done in a stirred solution of 0.1 M sodium salicylate, as the latter is a very good counterion for CTAB [48]. The best method was found to be application of a potential of −1.2 V for 1 min and then scanning to −0.2 V. After this procedure the electrode was dipped into a stirred 1 M KBr solution for 1 min without potential.

The dependence of the reoxidation current on the deposition time gives a linear relation between current and time up to a period of 10 minutes. Longer times cause deviation from linearity due to reaching equilibrium conditions.

The dependence of the reoxidation current of titanium(IV) on the concentration applying proper preconcentration times is shown in Fig. 3. With a deposition time of 1 minute a linear curve is obtained from 10 to 250 $\mu g\ l^{-1}$ Ti(IV) and with 2 min deposition time linearity exists from 5 to 160 $\mu g\ l^{-1}$. When increasing the time of deposition up to 10 min, a linear range from 1 to

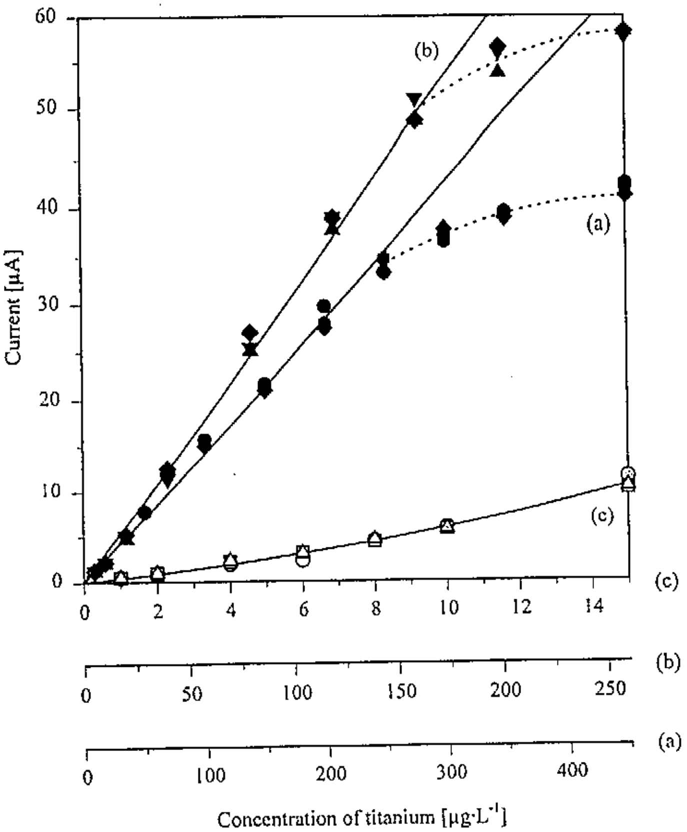

Fig. 3 Calibration plots for titanium with different preconcentration times; deposition times: (a) 1 min, (b) 2 min, (c) 10 min; other experimental parameters as in Fig. 2

10 $\mu g\,l^{-1}$ can be observed.

The relative standard deviation is 4.0 % for 5 repeated measurements (50 $\mu g\,l^{-1}$ Ti(IV), 2 min deposition time). The limit of detection (calculated as 3σ) of titanium is 0.46 $\mu g\,l^{-1}$ and 0.1 $\mu g\,l^{-1}$ with deposition times of 2 min and 10 min., respectively.

Interferences

Interferences of many cations and anions with the reoxidation signal of titanium(III) were examined.

Anions. Common anions like nitrate, sulfate, phosphate, and chloride do not interfere even in a 500 fold mass-excess with respect to titanium (Table I).

The presence of a 500 fold excess of bromide results in slightly increasing background currents without changing the signal. The same excess of iodide leads to a diminution of the titanium signal by about 32 %. This decrease is due to the fact that iodide is a very good counterion for CTAB micelles, because of its small hydrated ionic radius; competitive attraction between titanyl oxalate and iodide is the consequence. Fluoride already interferes at a 5 fold excess, owing to complexation of Ti(IV). Salicylate interferes by increasing the background current and decreasing the signal of titanium. This is obviously due to competitive concurrence for the ion exchanging groups. Vanadate and molybdate are complexed by oxalate forming ion pairs with CTAB; molybdate additionally yields an electrochemical response overlapping with the signal of titanium. Tungsten(VI) interferes severely.

Chromate and permanganate act as oxidizing agents for titanium(III), and therefore decrease its reoxidation currents.

Cations: Electroactive metal cations, which are reduced to the elemental state at a potential of -1.2 V, are accumulated onto the electrode surface (Table II).

In the case that they do not form anionic oxalate complexes, they interfere significantly at 50 fold excess only, if the resulting electrochemical response overlaps with the reoxidation of Ti(III). At higher concentrations they show a decreasing effect on the titanium signal, if they are deposited on the electrode surface, because they reduce the available lipophilic surface area. Indium, thallium and copper form stable anionic oxalate complexes and give a reoxidation peak as well. Their preconcentration probably proceeds *via* direct electrolytic reduction as well as *via* the complex; they interfere at higher concentrations. Cobalt, nickel, zinc, aluminum, iron(III), uranium(VI), vanadium(IV), zirconium(IV), and gallium(III) are accumulated as anionic oxalate-complexes resulting in a decrease of the titanium reoxidation response. Chromium(III), manganese(II) and antimony(V) do not interfere severely up to a 50 fold excess, because they do not form anionic oxalate complexes.

Table I Influence of anionic interferences on the determination of titanium: supporting electrolyte: 0.05 M acetate buffer, 0.01 M oxalic acid and 0.1 mM CTAB; 100 $\mu g\ l^{-1}$ titanium(IV); deposition time: 2 min; voltammetry: DPV, initial potential -1.2 V, final potential 0.0 V, scan rate 10 $mV\ s^{-1}$

Interferent	Added as	Change of peak current [±%] concentration of interferent		
		0.5 $mg\ l^{-1}$	5 $mg\ l^{-1}$	50 $mg\ l^{-1}$
AsO_2^-	$NaAsO_2$	±0	±0	-15
AsO_3^-	$NaHAsO_4$	±0	±0	-15
Br^-	KBr	±0	±0	±0 (b)
Cl^-	NaCl	±0	±0	±0
$Cr_2O_7^{2-}$	$K_2Cr_2O_7$	-48 (c)	-	-
F^-	NaF	-23	-58	-88
I^-	NaI	±0	±0	-32
MnO_4^-	$KMnO_4$	-66 (c)	-	-
MoO_4^{2-}	$(NH_4)_6Mo_7O_{24}$	(a)	(a)	(a)
NO_3^-	$NaNO_3$	±0	±0	±0
PO_4^{3-}	Na_3PO_4	±0	±0	±0
SO_4^{2-}	Na_2SO_4	±0	±0	±0
Salycilate $HOC_6H_4COO^-$	Na-salycilate	±0	-10 (c)	-65 (c)
VO_3^-	NH_4VO_3 in 0.3 M HNO_3	-30	-100	-100
WO_4^{2-}	Na_2WO_4	-21	-90	-100

(a) overlapping signals
(b) increasing backround current
(c) decreasing with increasing number of scans

Sample

The method proposed was employed for determination of titanium in a mineral sample (stone-wool), where it is present as TiO_2. The sample containing SiO_2, Al_2O_3, Fe_2O_3, CaO, MgO, Na_2O and TiO_2 and small amounts of other oxides was digested with an equimolar mixture of sodium and potassium carbonate as described above. Control analyses were performed with inductively coupled

Table II Influence of cationic interferences on the determination of vanadium. Experimental parameters as in Table IV

Interferent	Added as	Change of peak current [±%] concentration of interferent		
		$0.5\ \mathrm{mg\,l^{-1}}$	$5\ \mathrm{mg\,l^{-1}}$	$50\ \mathrm{mg\,l^{-1}}$
Ag^+	$AgNO_3$ in 0.5 M HNO_3	±0	-25	-100
Al^{3+}	$AlCl_3$	-67	-100	-100
Cd^{2+}	$CdCl_2$	±0	±0	(a)
Co^{2+}	$CoCl_2$	±0	-20	-100
Cr^{3+}	$CrCl_3$	±0	-9	-31
Cu^{2+}	$CuCl_2$	-25	-42	-56
Fe^{3+}	$FeCl_3$ in 15% HCl	-14	-57	-97
Ga^{3+}	$Ga(NO_3)_3$	-38	-92	-100
Hg^{2+}	$Hg(NO_3)_2$ in diluted HNO_3	+6	-45	-54
In^{3+}	$In(NO_3)_3$	-22	-71	-100 (a)
Mn^{2+}	$MnCl_2$	±0	±0	-27
Ni^{2+}	$NiCl_2$	±0	-37	-100
Pb^{2+}	$Pb(NO_3)_2$ in diluted HNO_3	(a)	(a)	(a)
Sb^{3+}	$SbCl_3$	±0	±0	-20
Sb(V)	$SbCl_5$ in 10 M HCl	±0	-15	-100
Sn(IV)	$SnCl_4$ in HCl	-20	-63	(a)
Tl^{3+}	$TlCl_3$	±0	-53	-100 (a)
UO_2^{2+}	$UO_2(acetate)_2$	-51	-86	-100 (a)
VO^{2+}	$VOSO_4$	-20	-90	-100
Zn^{2+}	$ZnSO_4$	±0	-50	-100
ZrO^{2+}	$ZrOCl_2$	-30	-100	-100

Table III Determination of titanium in a mineral sample (stone wool)

Sample	Voltammetry [TiO_2] [%± relative standard deviation]	ICP-MS [TiO_2] [%± relative standard deviation]
Sample 1	3.6 ± 0.2 (3)*	3.62 ± 0.03
Sample 2	3.7 ± 0.2 (3)*	3.72 ± 0.04
Mean value	3.6 ± 0.2	3.67 ± 0.04

* Number of repeated measurements

plasma mass spectrometry ICP-MS. Table III shows the results. Although the electrochemical method shows higher relative standard deviations, the agreement between the different methods is satisfactory.

Vanadium

Oxalate is a very suitable ligand for chelation of vanadium(V), since it forms a rather stable bisoxalato-dioxo-vanadate(V) complex in acidic solution [49]. The formation constant is 1.8×10^9 $\text{mol}^{-2}\,\text{l}^2$ according to Eq. (8)

$$VO_2^+ + 2(C_2O_4)^{2-} \rightleftharpoons [VO_2(C_2O_4)_2]^{3-} \tag{8}$$

Formation of the monooxalate complex proceeds only to a small extent.

Figure 4 shows the electrochemical behavior of the dioxalate complex on a CPE. Vanadium(IV) and (V)-oxalate solutions produce identical cyclic voltammograms.

In the presence of V(V) reduction of $[VO_2(Ox)_2]^{3-}$ at around +0.4 V and oxidation at around +0.64 V are clearly discernible in the voltammogram (curve b). Both electrochemical reactions can be described by Eq. (9)

$$[VO_2(Ox)_2]^{3-} + 2H^+ + e^- \rightleftharpoons [VO(Ox)_2]^{2-} + H_2O \tag{9}$$

The peak currents are rather small and do not show any dependence on the accumulation time. If applying differential pulse voltammetry with an unmodified electrode, the practically achievable detection limit for the direct determination of the vanadium oxalate complex is around 0.5 $\text{mg}\,\text{l}^{-1}$ V and is not suitable for the determination of traces of vanadium.

If cetyltrimethylammonium bromide is present in the solution in concentrations around and above the CMC, vanadium oxalate becomes preconcentrable at the electrode surface yielding a pronounced reduction and

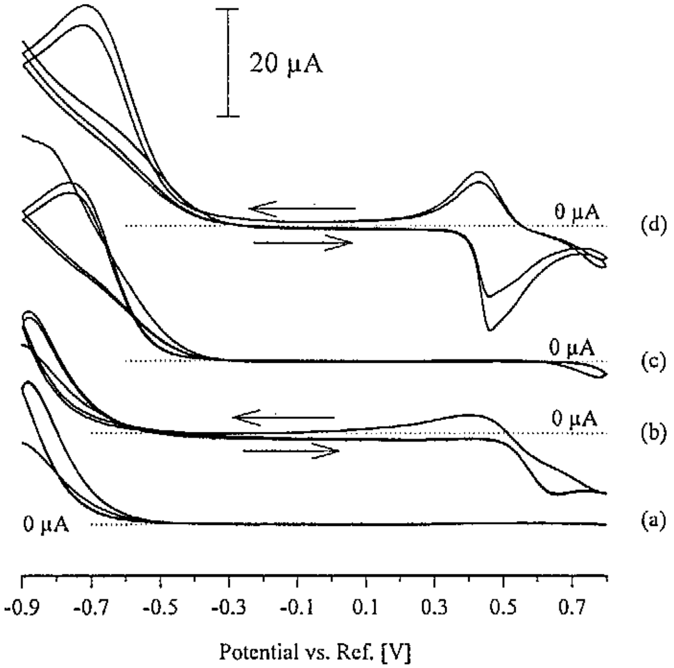

Fig. 4 Cyclic voltammograms of vanadium(V) at a plain (a,b) and a CTAB-modified (c,d) carbon paste electrode; equilibration time 30: s, initial potential: -0.9 V, final potential: +0.8 V, scan rate: 20 mV s^{-1}; supporting electrolyte: 0.01 M oxalic acid; V(V) as vanadate: (a, c) 0, (b) 10, (d) 1 mg l^{-1} V(V); CTAB: (a, b) 0, (c, d) 0.25 mM

reoxidation signal of the redox couple $[VO_2(Ox)_2]^{3-}/[VO(Ox)_2]^{2-}$ with an enormous enhancement in peak currents (Fig. 4, curve d). The electrode reaction is reversible, the oxidation potential shifted to less positive values. The reduction occurs at +0.4 V, reoxidation at +0.45 V.

Other cationic ion-paring reagents did not show any pronounced effect on the preconcentration of vanadium. Obviously CTAB tends to form lipophilic ion congregates with vanadium oxalate, whereas the other surfactants under investigation show only a very limited affinity towards the target analyte.

Vanadium as an oxalate complex can be preconcentrated onto the surface of CPEs in the presence of CTAB, particularly if negative deposition potentials are applied. This can be shown also by accumulating V(V) from an identical solution under open circuit conditions; in this case it is also preconcentrable, but only to a very small extent requiring at least 1 mg l^{-1} V(V). Thus, the principle of the accumulation process is rather the same as that found for titanium oxalate. The preconcentration is performed by *in situ* formation of an ion-exchanger at the electrode surface (process A), and by formation of ion-pairs or micellar congregates in solution (process B) according to Eqs (10)–(13).

(A)

$$[\mathrm{CTA}]^{+}_{x,mic.,sol.} \xrightarrow{-0.9\,\mathrm{V}} [\mathrm{CTA}^{+}]_{x,mic.,surf.} \tag{10}$$

$$[\mathrm{CTA}^{+}]_{x,mic.,surf.} + y[\mathrm{VO_2(C_2O_4)_2}]^{3-}_{sol.} \longrightarrow \left\langle [\mathrm{CTA}^{+}]_x \{[\mathrm{VO_2(C_2O_4)_2}]^{3-}\}_y \right\rangle_{surf} \tag{11}$$

(B)

$$[\mathrm{CTA}^{+}]_{x,mic.,sol.} + y[\mathrm{VO_2(C_2O_4)_2}]^{3-}_{sol.} \longrightarrow \left\langle [\mathrm{CTA}^{+}]_x \{[\mathrm{VO_2(C_2O_4)_2}]^{3-}\}_y \right\rangle_{sol.} \tag{12}$$

$$\left\langle [\mathrm{CTA}^{+}]_x \{[\mathrm{VO_2(C_2O_4)_2}]^{3-}\}_y \right\rangle_{sol.} \xrightarrow{-0.9\,\mathrm{V}} \left\langle [\mathrm{CTA}^{+}]_x \{[\mathrm{VO_2(C_2O_4)_2}]^{3-}\}_y \right\rangle_{surf.} \tag{13}$$

When applying a negative potential to promptly increased adsorption of CTA$^+$ at the electrode surface, the vanadium oxalate anion will be reduced simultaneously during accumulation (Eq. (14)). As indicated, bisoxalato-oxo-vanadate(IV) will therefore be immobilized at the electrode-solution interface.

$$\begin{aligned} &\left\langle [\mathrm{CTA}^{+}]_x \{[\mathrm{VO_2(C_2O_4)_2}]^{3-}\}_y \right\rangle_{surf.} + 2y\mathrm{H}^{+} + y\mathrm{e}^{-} \xrightarrow{-0.9\,\mathrm{V}} \\ &\qquad \left\langle [\mathrm{CTA}^{+}]_x \{[\mathrm{VO_2(C_2O_4)_2}]^{2-}\}_y \right\rangle_{surf.} + y\mathrm{H_2O} \end{aligned} \tag{14}$$

In principle, DPVs can be recorded in both anodic and cathodic direction yielding a response for vanadium, but scanning in anodic direction is preferable. When measuring the reduction signal of vanadium(V) the current is in fact 20 times higher than without CTAB, but preconcentration of CTA$^+$ at positive potentials is not so effective, because hydrophobic attraction between the lipophilic part of the surfactant and the electrode surface must overcome the electrostatic repulsion. Scanning in anodic direction even results in much higher peak currents. Negative potentials show a favorable effect on the preconcentration of the surfactant. Figure 5 shows a few sample voltammograms in anodic DPV mode.

At −0.6 V the reduction of oxygen containing functional groups on the carbon surface appears (pronounced in the presence of CTAB); the reoxidation of V(IV) occurs at +0.44 V.

As expected the peak currents increase with increasing negative deposition potentials, since adsorption of CTA$^+$ becomes more effective. The optimum for deposition is found at a potential of −0.9 V. When applying a more negative voltage the peak current decreases sharply probably due to reduction of vanadium(V) to oxidation states lower than IV; such species do not form very

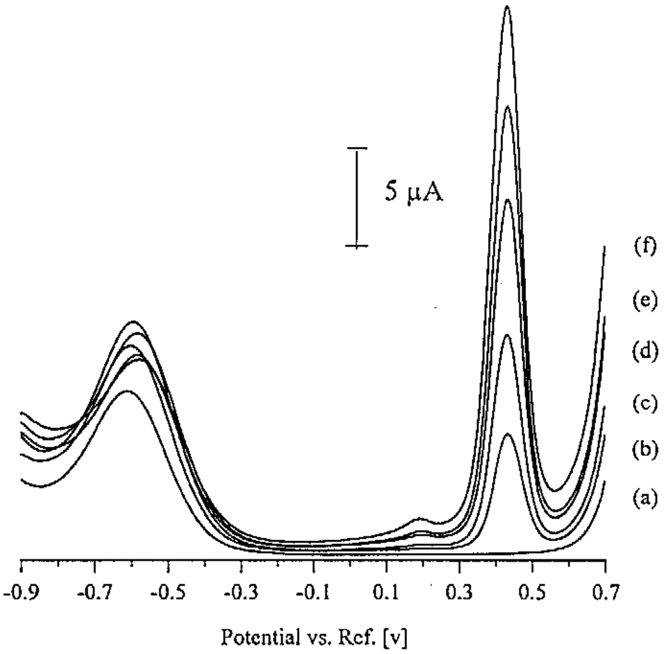

Fig. 5 Differential pulse voltammograms of V(V) with a CPE modified *in situ* with CTAB; scan rate: 20 mV s^{-1}; supporting electrolyte: 0.01 M oxalic acid, 0.25 mM CTAB; deposition time: 1 min; deposition potential: −0.9 V; vanadium concentrations: (a) 0, (b) 20, (c) 40, (d) 60, (e) 80, (f) 100 μg l^{-1}

stable oxalate complexes.

The dependence of the peak current on the CTAB-concentration in solution shows a sharp maximum at 0.25 mM CTAB (CMC = 0.08 mM in the supporting electrolyte). Therefore it can be assumed that at concentrations lower than CMC either ion-pairing of CTA^+ individuals and vanadium oxalate or adsorption of CTA^+ monomers on the electrode surface control the preconcentration. As the optimum CTAB-concentration is significantly higher than CMC, transport of vanadium to the electrode surface via micellar aggregates contributes also to the accumulation process. When the CTAB-concentration is higher than 0.25 mM, the peak current decreases because of enhanced coverage of the electrode surface with the surfactant leading to a reduction of effective area.

Other parameters influencing the height of the vanadium(IV) oxidation signals are the composition and the pH of the measurement solution. The optimum concentration of oxalic acid was found to be between 0.01 and 0.0175 M. For all further investigations 0.01 M oxalic acid was taken as the supporting electrolyte.

The influence of pH (adjusted by hydrochloric acid or sodium hydroxide) shows a sharp maximum at a value of 2.2. At a pH of 1.0 no oxidation peak can be found anymore. This behavior can be explained by the fact that below pH 2 almost all of the oxalate ions in solution are fully protonated, whereas there is practically no $C_2O_4^{2-}$. On the other hand, VO_2^+ exists only in acidic solutions (pH < 3.5). As in our studies the concentration of V is very low, only monomeric species, particularly VO_2^+, have to be considered. Polyvanadates are formed only in more concentrated solutions. Varying the concentration of CTAB influences the pH optimum only slightly.

The potential of the peak is also strongly dependent on the hydrogen ion concentration in solution. It decreases linearly with decreasing H^+ concentration with a slope of 106 mV per pH unit. This suggests that two hydrogen ions are involved in the redox process according to Eq. (9).

The complete removal of accumulated vanadium oxalate from the CTA^+-modified electrode surface was performed with the same method as for titanium.

As the CTA^+ is preconcentrable at the electrode at negative potentials via electrostatic attraction, the reoxidation current of vanadium increases with increasing deposition time. With 20 μg l^{-1} V(V) there is a linear relation between current and time up to a period of 8 min, whereas 50 μg l^{-1} V(V) shows linearity up to 6 min. Longer times cause deviation from linearity due to reaching equilibrium conditions. When taking smaller concentrations of CTAB, the linear range can be extended to longer accumulation periods.

The dependence of the oxidation current of vanadium(IV) on the concentration applying different preconcentration times is shown in Fig. 6.

Linearity exists for a 1 minute's period from 5 to 200 μg l^{-1} V, for 2 min from 2.5 to 100 μg l^{-1} V. When increasing the time of deposition up to 10 min, a concentration of 0.5 μg l^{-1} V is practically determinable; linearity exists from 0.5 to 5 μg l^{-1} V.

The relative standard deviation is 3.5 % for 7 repetitive measurements (20 μg l^{-1} V, 1 min preconcentration). The detection limit calculated as 3σ for 1 min deposition time is 0.41 μg l^{-1} V, whereas it is 0.07 μg l^{-1} vanadium with 10 min.

Interferences

Anions: Addition of a 500 fold excess of bromide leads to diminution of the signal, the same amount of iodide yields an oxidation signal overlapping with the vanadium peak (Table IV).

The influence of fluoride is not serious, but diminution of the vanadium signal occurs with higher concentrations due to complexation. Salicylate interferes by decreasing the signal because of competitive concurrence for the ion exchanging groups. Molybdate forms an anionic oxalate complex that is ion-paired by CTA^+. Tungstate, chromate and permanganate interfere severely either

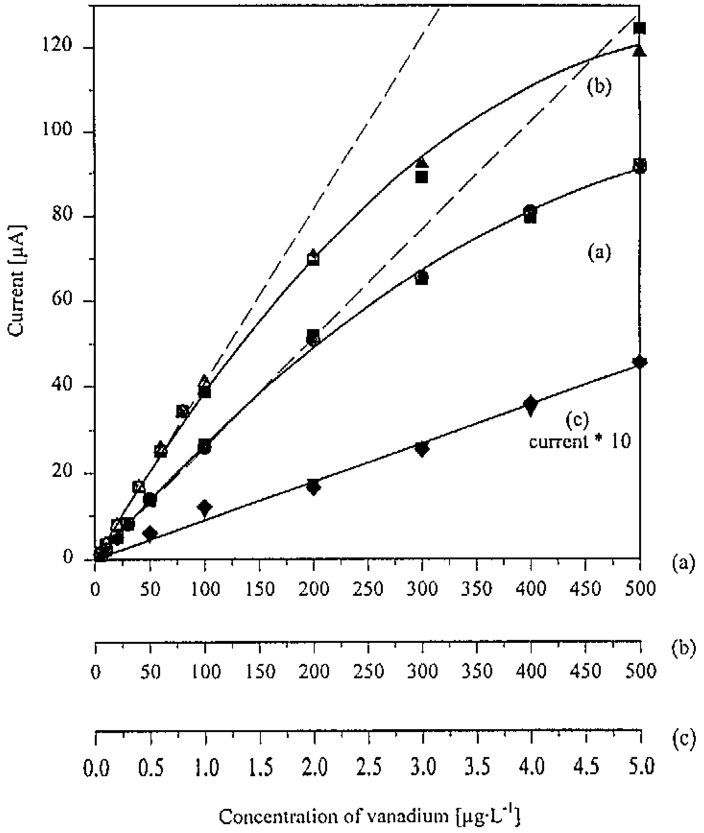

Fig. 6 Calibration plots for vanadium with different preconcentration times; deposition times: (a) 1 min, (b) 2 min, (c) 10 min; other experimental parameters as in Fig. 5; current axis of curve c 10 times expanded

by competitive interaction with the surfactant or by chemical reoxidation of the analyte.

Cations: All metal ions that form stable anionic oxalate complexes, i.e., Al^{3+}, Co^{2+}, Cu^{2+}, Fe^{3+}, Ga^{3+}, Ni^{2+}, TiO^{2+}, Tl^{3+}, UO_2^{2+}, and ZrO^{2+}, interfere severely at a 50 fold mass excess, Zn^{2+}at a 500 fold excess, by concurring ion-paring with CTA^+ (Table V).

Copper and iron produce an overlapping signal at higher concentrations. Silver, mercury, cadmium, lead, tin, thallium, and antimony(III) will be reduced to the elemental state on the electrode surface at −0.9 V. They do not interfere severely up to a 50 fold mass excess. Chromium(III) and manganese(II) can be present even at high concentrations, because they do not form anionic complexes with oxalate. Sb(V), TiO^{2+}, and ZrO^{2+} form precipitates in solution and disturb the determination of vanadium.

Table IV Influence of anionic interferences on the determination of vanadium. Supporting electrolyte: 0.01 M oxalic acid and 0.25 mM CTAB; 100 μg l^{-1} vanadium(V) as vanadate; deposition time: 1 min; deposition potential: −0.9 V; voltammetry: DPV, initial potential −0.9 V, final potential +0.7 V, scan rate 20 mV s^{-1}

Interferent	Added as	Change of peak current [±%]		
		Concentration of interferent		
		0.5 mg l^{-1}	5 mg l^{-1}	50 mg l^{-1}
AsO_2^-	$NaAsO_2$	±0	±0	±0
AsO_3^-	$NaHAsO_4$	±0	±0	±0
Br^-	KBr	±0	±0	-37
Cl^-	NaCl	±0	±0	±0
$Cr_2O_7^{2-}$	$K_2Cr_2O_7$]	-51	-100	-100
F^-	NaF	±0	-6	-37
I^-	NaI	±0	±0	§
MnO_4^-	$KMnO_4$	-40	-47	-86
MoO_4^{2-}	$(NH_4)_6Mo_7O_{24}$	-33	-91	-100
NO_3^-	$NaNO_3$	±0	±0	-15
PO_4^{3-}	Na_3PO_4	±0	±0	±0
SO_4^{2-}	Na_2SO_4	±0	±0	-13
Salicylate $HOC_6H_4COO^-$	Na-salicylate	±0	-11	-61
WO_4^{2-}	Na_2WO_4	-11	-40	-100

§ overlapping signals

Sample

The proposed method was employed for the determination of vanadium in a fuel oil sample, where vanadium is present in the form of organometallic complexes with porphyrins and with other organic ligands. Dry calcination was applied as the most suitable mineralization procedure for the voltammetric determination, because other methods will not oxidize the organic material completely. Control analyses were performed with ICP-MS (Table VI). The agreement of results between the voltammetric and the reference method is very good.

Table V Influence of cationic interferences on the determination of vanadium; experimental parameters as in Table IV

Interferent	Added as	Change of peak current [±%]		
		Concentration of interferent		
		0.5 mg l^{-1}	5 mg l^{-1}	50 mg l^{-1}
Ag^+	$AgNO_3$ in 0.5 M HNO_3	±0	-27	-100
Al^{3+}	$AlCl_3$	-58	-97	-100
Cd^{2+}	$CdCl_2$	±0	-9	-19
Co^{2+}	$CoCl_2$	-10	-16	-100
Cr^{3+}	$CrCl_3$	±0	±0	±0
Cu^{2+}	$CuCl_2$	-10	-31	§
Fe^{3+}	Fe^{3+} in 15% HCl	-50	-97	§
Ga^{3+}	$Ga(NO_3)_3$	-37	-100	-100
Hg^{2+}	$Hg(NO_3)_2$ in diluted HNO_3	-10	-40	-86
In^{3+}	$In(NO_3)_3$	-22	-74	-100
Mn^{2+}	$MnCl_2$	±0	-18	-30
Ni^{2+}	$NiCl_2$	±0	-14	-100
Pb^{2+}	$Pb(NO_3)_2$ in diluted HNO_3	±0	±0	±0
Sb^{3+}	$SbCl_3$	±0	-37	-100
Sb(V)	$SbCl_5$ in 10 M HCl	±0	-50	-100
Sn(IV)	$SnCl_4$ in HCl	-14	-55	-100
TiO^{2+}	$TiCl_4$ in 5 M HCl	-22	-100	-100
Ti^{3+}	$TiCl_3$	-5	-48	-100
UO_2^{2+}	$UO_2(acetate)_2$	±0	§	§
Zn^{2+}	$ZnSO_4$	±0	-7	-100
ZrO^{2+}	$ZrOCl_2$	-14	-90	-100

§ overlapping signals.

Table VI Determination of vanadium in a fuel oil sample

Sample	Voltammetry [μg g^{-1} ± relative standard deviation]	ICP-MS [TiO_2] [μg g^{-1} ± relative standard deviation]
Sample 1	49.5 ± 1.2 (3)*	49.94 ± 0.89
Sample 2	48.5 ± 1.5 (3)*	50.21 ± 0.03
Mean value	49.0 ± 1.5	50.10 ± 0.90

* Number of repeated measurements.

Molybdenum

Molybdate in neutral or basic solution of various supporting electrolytes does not show any electrochemical response in cyclic voltammograms within the applied potential range from −1.2 to +0.8 V. In acidic solutions (sulfuric, hydrochloric, or acetic acid) a broad reduction signal at around −0.62 V and oxidation at −0.47 V can be observed (Fig. 7b).

Compared to data from the literature, assignment of these responses to the reduction of Mo(VI) to Mo(V) and its reoxidation seems probable [50].

When using oxalic acid as a supporting electrolyte, the changes in the cyclic voltammograms are drastic (Fig. 7d): The reduction is not distinctly discernible and seems to be shifted to more negative potentials, whereas oxidation can be observed at +0.65 V. The occurrence of the oxidation peak is dependent on the negative vertex potential, since the signal appears only if the scan is run to less than −0.5 V; it does not show any dependence on the preconcentration time. Therefore, it can be concluded that in the presence of oxalate the reduction is shifted to more negative potentials, whereas the oxidation is shifted to more positive potentials; the electrochemical redox reaction thus becomes more irreversible. Most commonly formation of a stable 1:1 complex of Mo(VI) and oxalate is assumed having a formation constant of 6.3×10^{13} mol^{-3} l^{3} according to Eq. (15) [51].

$$MoO_4^{2-} + C_2O_4^{2-} + 2H^+ \rightleftharpoons [MoO_3(C_2O_4)]^{2-} + H_2O \tag{15}$$

More detailed investigations of the complex formation between molybdenum(VI) and oxalate showed that two more complexes, $[Mo_2O_5(Ox)_2]^{2-}$ and $[Mo_2O_5(OH)(Ox)_2]^{3-}$, exist in solution in the pH range 2–7; the main species at pH 2 was found to be $[Mo_2O_5(Ox)_2]^{2-}$ in equimolar solution of molybdenum and oxalate [52].

Which type of complex provokes the oxidation signal at +0.65 V in the presence of oxalic acid is not clear. However, the signal is rather small and

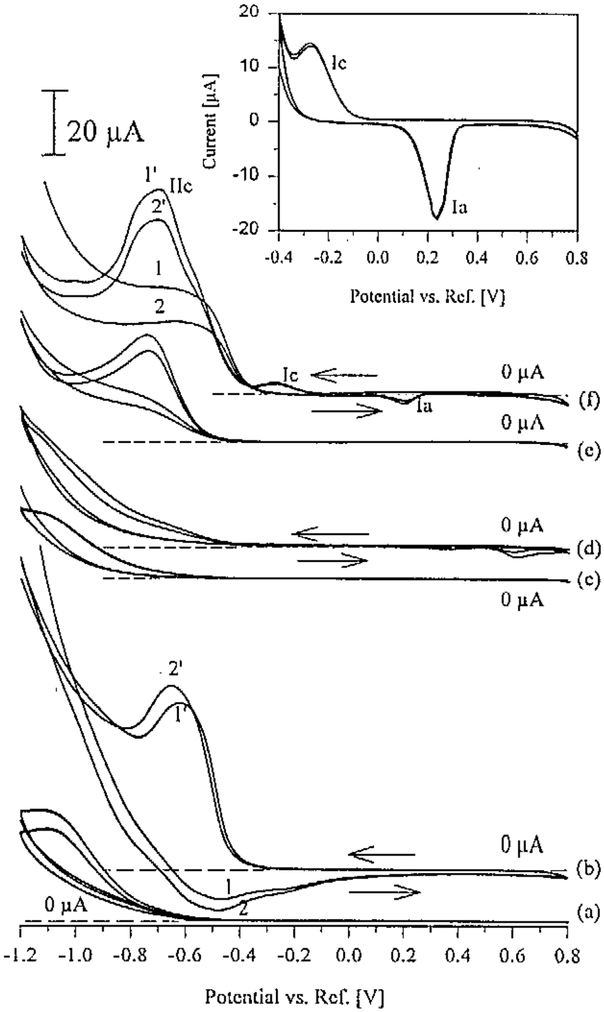

Fig. 7 Cyclic voltammograms of molybdenum(VI) at a plain (a,b,c,d) and a CTAB-*in situ* modified carbon paste electrodes (e,f); equilibration time: 30 s, initial potential: −1.2 V, final potential: +0.8 V, scan rate: 20 mV s^{-1}; supporting electrolyte: (a, b) 0.01 M HCl, (c, d, e, f) 0.01 M oxalic acid; Mo(VI) as molybdate: (a, c, e) 0, (b,d) 10, (f) 1 mg l^{-1}Mo(VI); CTAB: (a, b, c, d) 0, (e, f) 0.075 mM. Insert: initial potential: -0.4 V; other conditions as for (f)

cannot be exploited for trace determinations of molybdenum.

In the presence of CTAB the electrochemical activity of molybdenum(VI) complexed with oxalate shows a completely different behavior. In the cyclic voltammogram in the potential range between −1.2 and +0.8 V mainly two peaks in cathodic direction (Ic, IIc) and one oxidation signal in the anodic scan (Ia) can be observed (Fig. 7f). Signal Ic is much smaller than the signal occurring at more negative potential (IIc), but it is well developed and not superimposed by other signals. Oxidation IIa is obviously the reverse reaction of Ic, since it also appears, when the vertex potential is -0.4 V only (Fig. 7, insert). The corresponding potentials of Ic and Ia are -0.28 and +0.22 V. Peak IIc probably represents an overlap of at least two signals with the blank peak at around -0.7 V.

More details on the electrochemical processes occurring at the electrode surface can be seen in the DPVs recorded in both anodic and cathodic directions (Fig. 8).

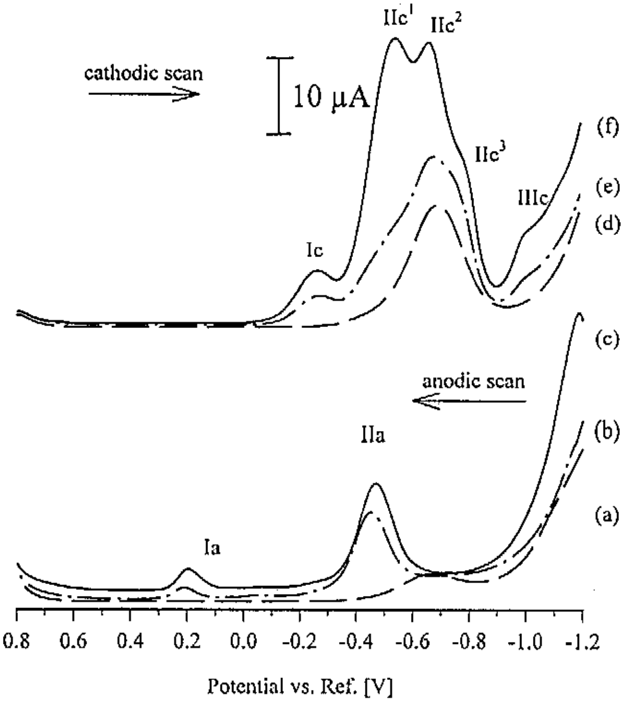

Fig. 8 Differential pulse voltammograms of Mo(VI) in anodic (a-c) and cathodic (d-f) direction with a CPE modified *in situ* with CTAB; initial potential: (a-c) -1.2 V, (d-f) +0.8 V; final potential: (a-c) +0.8 V, (d-f) -1.2 V; scan rate: 20 mV s^{-1}; supporting electrolyte: 0.01 M oxalic acid, 0.075 mM CTAB; deposition time: 2 min; deposition potential: (a-c) -1.2 V, (d-f) +0.8 V; molybdenum concentrations: (a,d) 0, (b,e) 0.5, (c,f) 1 mg l^{-1} Mo(VI)

In the scan in the cathodic direction peak Ic is clearly discernible at -0.25 V. Peak IIc, which was unresolved in the cyclic voltammogram is split into two signals (IIc^1, IIc^2 at -0.53 and -0.65 V, resp.) and also exhibits a shoulder (IIc^3). An additional small peak is found at around -1.0 V (IIIc). This indicates strongly that more than one molybdenum oxalate species exist in solution, which are reduced at different potentials. The signals depending on the Mo concentration, i.e. Ic, IIc^1, IIc^3, and IIIc, can thus be assigned to the reduction of either different species of Mo(VI) oxalate complexes, or to further reduction of formerly reduced species. Since these peaks occur only in the presence of CTAB, the cause for facilitating the electrochemical reaction must be a formation of ion-pairs at the electrode surface. Obviously, the lipophilic positive counterion compensates the negative charge of the Mo-complexes and thus allows the aggregate to overcome the electrostatic repulsion more easily.

Peak IIc^1 shows a dependence of the peak potential on pH and can therefore be ascribed most probably to the reduction of $[MoO_3(Ox)]^{2-}$ to the pentavalent species $[MoO_2(Ox)]^-$ (Eq. (16)).

$$\begin{array}{l} (CTA)_2[MoO_3(Ox)]_{surf} + 2H^+ + e^- \longrightarrow CTA[MoO_2(Ox)]_{surf} + CTA^+ + H_2O \\ \qquad\qquad\qquad\qquad\qquad\qquad \uparrow\downarrow \text{ probable dimerization?} \qquad (16) \\ \qquad\qquad\qquad\qquad\qquad\qquad (CTA)_2[Mo_2O_4(Ox)_2]_{surf} \end{array}$$

Peak IIc^2 corresponds to the signal of the blank, which is attributable to the reduction of carbon-oxygen functional groups of the electrode surface. The responses IIc^3 and IIIc are probably caused by molybdenum(VI) oxalate complexes of minor occurrence. To which extent possible catalytic reductions of H^+ are involved in the electrochemical response is not discernible from the voltammogram.

The potential of peak Ic shows practically no dependence on pH and must therefore be assigned to the reduction of a Mo species without involvement of protons. The response is dependent on the concentration of Mo. Most probable is an assignment to the reduction of the species $[Mo_2O_5(Ox)_2]^{2-}$ to a mixed valence compound according to Eq. (17)

$$\begin{array}{l} (CTA)_2[Mo_2O_5(Ox)_2]_{surf} + e^- + CTA^+ \xrightarrow{-0.4\ V} (CTA)_3[Mo^{V}Mo^{VI}O_5(Ox)_2]_{surf.} \\ \qquad\qquad\qquad\qquad\qquad\qquad\qquad \uparrow\downarrow \qquad\qquad\qquad (17) \\ \qquad\qquad\qquad\qquad (CTA)_2[MoO_3(Ox)]\cdot CTA[MoO_2(Ox)]_{surf} \end{array}$$

The primary product formed by the electron transfer can either be present as a stable mixed-valence complex, or disintegrate into the individual hexa- and pentavalent Mo compound; it is not yet clear, which alternative occurs at the electrode surface. Anyway, further reduction of the Mo(VI) must occur at more negative potentials.

In the scan in the anodic direction only two signals can be observed (Ia at +0.2 V, IIa at -0.48 V). The dependence of the potential of IIa on pH is at around 100 mV per pH unit and thus suggests the oxidation of Mo(V) oxalate to Mo(VI) oxalate (reverse reaction of Eq. (16)); probably it is the superimposition of more than one reaction. The potential of signal Ia does not show any dependence on pH; it obviously represents the reverse reaction of Eq. (17). Additionally it has to be considered that the peak currents of the redox pair Ic/Ia increase considerably when the negative vertex potential in the cyclic voltammogram is shifted anodically (Fig. 7, insert) indicating that the anionic mixed valence compound from Eq. (17) is rather stable. On applying more negative vertex potentials, the further reduction will decrease the available amount of the Mo(V)/Mo(VI) species.

Signal Ia in differential pulse voltammograms is linearly dependent on the molybdenum concentration and on the preconcentration time. Though its current is lower than that of peak IIa, it is better exploitable for analytical purposes, since IIa is not linearly dependent on concentration and does not show a pronounced dependence on preconcentration time. Therefore, peak Ia was exploited for all quantitative determinations.

Accumulation of molybdenum as an oxalate complex in the presence of CTAB is possible under closed and open circuit conditions; but it is much more effective if negative deposition potentials are applied. The accumulation process can again be explained by the formation of lipophilic ion-pairs on the one hand, and by the *in situ* formation of an ion-exchanger at the electrode surface by adsorption of the surfactant especially at negative potentials on the other hand. When scans in the anodic direction are run, simultaneous reduction of the Mo-oxalate occurs according to Eq. (17), and the mixed valence complex is the accumulated species. Other cationic ion-pairing reagents did not have the same effects as CTAB. The presence of these counterions in solution did not change the voltammograms of molybdenum oxalate alone. Obviously, they do not show a pronounced tendency to form ion-pairs with the target analyte.

The voltammograms for quantitation were recorded in anodic direction, as preconcentration of CTA^+ at positive potentials is not effective. The reoxidation signal Ia, recorded in the anodic scan, is thus well exploitable and shows much higher peak currents than the corresponding reduction peak Ic.

Figure 9 shows a few sample voltammograms in anodic DPV mode.

The dependence of the signal Ia on the deposition potential is investigated and a pronounced maximum at −0.4 V and a smaller at −0.9 V were found. At potentials > −0.2 V the Mo(VI) oxalate is not reduced and therefore yields no reoxidation peak. A potential of −0.4 V is the optimum voltage for accumulating the mixed valence complex as an ion-pair. More negative potentials effect onward reduction and thus a decrease in the accumulated amount of analyte. The second small maximum at −0.9 V is explainable by an increased adsorption of CTA^+ in that potential range

Variation of the CTAB concentration in solution shows the maximum response at 0.075 mM. This concentration is nearly equal to the CMC of CTAB. Apparently, the formation of micelles shows a disadvantageous effect on the accumulation of Mo onto the electrode. In contrast to the investigations with titanium and vanadium, where micelles contribute significantly to the transport

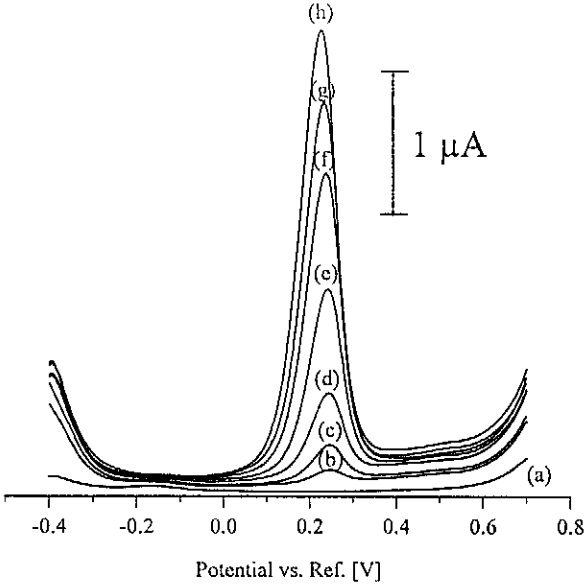

Fig. 9 Differential pulse voltammograms of Mo(VI) with a CPE modified *in situ* with CTAB; initial potential: −0.4 V, final potential: +0.7 V; scan rate: 20 mV s^{-1}; supporting electrolyte: 0.01 M oxalic acid, 0.075 mM CTAB; deposition time: 2 min; deposition potential: +0.4 V; molybdenum concentrations: (a) 0, (b) 5, (c) 10, (d) 20, (e) 40, (f) 60, (g) 80, (h) 100 μg l^{-1}

of the analyte towards the electrode surface, molybdate behaves differently. It seems that preferably individual aggregates between the oxalate complex and the counterions are adsorbed at the carbon paste interface, whereas there is only low affinity of the analyte towards CTA^+ micelles.

The optimum concentration of oxalic acid was found to be 0.01 M. Higher concentrations of oxalate seem to form aggregates with CTA^+ as well, which reduces the number of available counterions for the molybdenum complex.

Of major importance is the pH of the solution. the optimum formation of the target analyte species $[Mo_2O_5(Ox)_2]^{2-}$ occurs at pH 2, coinciding with a maximum preconcentration efficiency at this pH. Below pH 1 not sufficient $C_2O_4^{2-}$ ions are present as ligands in solution, whereas above pH 4.5 other species dominate.

Complete cleaning of the electrode surface was achieved by application of a potential of −1.2 V in a stirred solution of 0.005 M oxalic acid for 1 minute. Probably, molybdenum is completely reduced to lower oxidation states, of which the oxalate complexes do not show affinity to adhering CTA^+.

When varying the accumulation time, a linear dependence of the signal current is found for short periods. With 50 μg l^{-1} Mo(VI) there is a linear relation between current and time up to a period of 10 min, whereas 100 μg l^{-1} Mo(VI) show linearity up to 6 min.

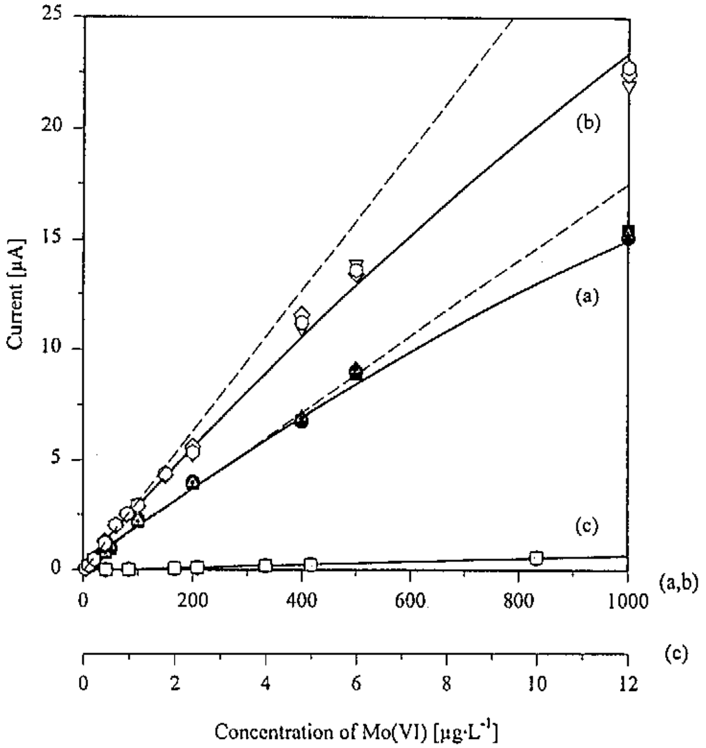

Fig. 10 Calibration plots for molybdenum with different preconcentration times; deposition times: (a) 1 min, (b) 2 min, (c) 10 min; other experimental parameters as in Fig. 9

The dependence of the oxidation current of molybdenum on the concentration applying different preconcentration times is shown in Fig. 10. Linearity exists for a 1 minute's period from 5 to 500 $\mu g\,l^{-1}$ Mo(VI), whereas it ranges from 2.5 to 200 $\mu g\,l^{-1}$ Mo for 2 min, and from 0.5 to 5 $\mu g\,l^{-1}$ Mo for 10 min.

The relative standard deviation is 3.9 % for 7 repetitive measurements (100 $\mu g\,l^{-1}$ Mo(VI), 2 min preconcentration). The practically achievable limit of detection is 5 $\mu g\,l^{-1}$ Mo(VI) with a deposition time of 1 min and 0.5 $\mu g\,l^{-1}$ Mo with 10 min. The detection limit as 3σ value was calculated as 0.33 $\mu g\,l^{-1}$ Mo(VI) for 1 min deposition and as 0.04 $\mu g\,l^{-1}$ Mo(VI) for 10 min.

Interferences

Anions: Anions such as nitrate, fluoride, chloride, sulfate, and phosphate reduce slightly the Mo signal in 500 fold mass excess (Table VII).

Similar effects are found for bromide, arsenite, and arsenate. Iodide in high excess gives a more pronounced diminution of the signal accompanied by

Table VII Influence of anionic interferences on the determination of molybdenum; supporting electrolyte: 0.01 M oxalic acid and 0.075 mM CTAB; 100 $\mu g\,l^{-1}$ molybdenum(VI) as molybdate; deposition time: 120 s, deposition potential: -0.4 V; voltammetry: DPV, initial potential -0.4 V, final potential +0.7 V, scan rate 20 mV s^{-1}

Interferent	Added as	Change of peak current [±%]		
		Concentration of interferent		
		0.5 mg l^{-1}	5 mg l^{-1}	50 mg l^{-1}
AsO_2^-	$NaAsO_2$	±0	-8.9	-17.8
AsO_3^-	$NaHAsO_4$	±0	-9.2	-20
Br^-	KBr	±0	-8.8	-35
Cl^-	NaCl	±0	±0	-24.1
$Cr_2O_7^{2-}$	$K_2Cr_2O_7$	-100	(a)	(a)
F^-	NaF	±0	±0	-32
I^-	NaI	±0	+7.2	-48.5
MnO_4^-	$KMnO_4$	-16.9	-40.4	(a)
NO_3^-	$NaNO_3$	±0	±0	-10.8
PO_4^{3-}	Na_3PO_4	±0	±0	-11.3
SO_4^{2-}	Na_2SO_4	±0	±0	-18
Salicylate $HOC_6H_4COO^-$	Na-salicylate	-12.8	-30.2	-58.3
VO_3^-	NH_4VO_3 in 0.3 M HNO_3	-15.1	-57.0	-100
WO_4^{2-}	Na_2WO_4	±0	-88.3	-100

(a) overlapping signals
(b) increasing backround current
(c) precipitation

an additional oxidation peak, which gradually overlaps with the molybdenum signal. This effect is even more pronounced with permanganate and dichromate. Other ions such as vanadate or tungstate compete for oxalate and CTA^+ and thus decrease the response of molybdenum completely in a 500 fold mass excess. Salicylate, which can act as counterion for CTA^+, also interferes, but molybdenum determinations are possible even at a 500 fold excess.

Cations: The influence of cations on the oxidation signal of molybdenum is summarized in Table VIII.

Cadmium(II), chromium(III), manganese(II), antimony(III), and lead(II)

Table VIII Influence of cationic interferences on the determination of molybdenum; experimental parameters as in Table VII

Interferent	Added as	Change of peak current [±%]		
		concentration of interferent		
		0.5 mg l^{-1}	5 mg l^{-1}	50 mg l^{-1}
Ag^+	$AgNO_3$ in 0.5 M HNO_3	-22.8	-57	(a)
Al^{3+}	$AlCl_3$	-11 (b)	-48.5	-82 (a)
Cd^{2+}	$CdCl_2$	±0	±0	-4.7
Co^{2+}	$CoCl_2$	±0	-10.8	-68.4
Cr^{3+}	$CrCl_3$	-9.7	-26.1	-39.5
Cu^{2+}	$CuCl_2$	±0 (b)	(a)	(a)
Fe^{3+}	$FeCl_3$ in 15% HCl	±0	-15 (b)	-57
Ga^{3+}	$Ga(NO_3)_3$	-25.8	-72.5	-91.6 (c)
Hg^{2+}	$Hg(NO_3)_2$ in diluted HNO_3	(a)	(a)	(a)
In^{3+}	$In(NO_3)_3$	±0	-10.8	-7
Mn^{2+}	$MnCl_2$	±0	±0	-30
Ni^{2+}	$NiCl_2$	-10.6	-23.4	-88.3
Pb^{2+}	$Pb(NO_3)_2$ in diluted HNO_3	±0	±0	-7.5
Sb^{3+}	$SbCl_3$ in 0.5 M HCl	±0	-12.5	-50
Sb(V)	$SbCl_5$ in 10 M HCl	±0	-36.5	-100 (c)
Sn(IV)	Sn(IV) in HCl	-19.1	-54.3	-100 (c)
TiO^{2+}	$TiCl_4$ in 5 M HCl	-82.1	-100	-100 (c)
Tl^{3+}	$TlCl_3$	-24.5 (b)	-56.9	-100
UO_2^{2+}	$UO_2(acetate)_2$	-24.7	-46.2	-67.0
VO^{2+}	$VOSO_4$	-12	-50	-100
Zn^{2+}	$ZnSO_4$	±0	-17.6	-100
ZrO^{2+}	$ZrOCl_2$	-42.7	-85.4	-100

(a) overlapping signals
(b) increasing backround current
(c) precipitation

allow determination of Mo(VI) even at high concentrations of the interferent. A 50 fold excess of Al^{3+}, Fe^{3+}, Co^{2+}, Ni^{2+}, In^{3+}, UO_2^{2+} and Zn^{2+} leads to minor signal decrease, and even at a 500 fold mass excess exploitation of the molybdenum signal is possible in most cases. The presence of a 50 fold mass excess of Ga^{3+}, Tl^{3+}, TiO^{2+}, VO^{2+} and ZrO^{2+}, which are also known to form stable anionic oxalate complexes, produces severe signal decrease by concurring ion-pairing with CTA^+. Copper, silver, and mercury cause peak overlaps at higher concentrations, since they are reduced to the elemental state at −0.4 V and reoxidized during the scan. Ga(III), Sb(V), Sn(IV), and Ti(IV) form precipitates in solution with CTAB when added at a 500 fold mass excess and disturb the determination of molybdenum.

Sample

The method was employed for the determination of molybdenum in steel. Acid digestion was applied for the dissolution of the sample. It was found that a 300 fold excess of iron in the standards improved the results, since otherwise the obtained data were 10 % too low.

Control analyses were performed with ICP-MS (Table IX). The agreement of results between the voltammetric and the reference method is very good.

Table IX Determination of molybdenum in a steel sample

Sample	Voltammetry [%± standard deviation]	ICP-MS [%± standard deviation]
Sample 1	0.241 ± 0.007 (3)*	0.243 ± 0.005
Sample 2	0.235 ± 0.011 (3)*	0.225 ± 0.010
Mean value	0.238 ± 0.011	0.234 ± 0.010

* Number of repeated measurements.

Conclusion

The voltammetric methods using a CTAB *in situ* modified carbon paste electrode as described in this paper are very good analytical procedures for the determination of trace levels of titanium, vanadium, and molybdenum. They are well applicable to the determination of the elements in real samples.

Acknowledgements

The authors wish to acknowledge support of this work by the Austrian Fonds zur Förderung der Wissenschaftlichen Forschung, FWF, project #P11172-CHE.

References

1. Vydra F., Štulík K., Juláková E.: *Electrochemical Stripping Analysis*, Wiley, New York 1976.
2. Lingane J.J., Kennedy J.H.: Anal. Chim. Acta **15**, 295 (1956).
3. Pecsok R.L.: J. Amer. Chem. Soc. **73**, 1304 (1950).
4. Pecsok R.L., Maverick E.F.: J. Amer. Chem. Soc. **76**, 358 (1953).
5. Headridge J.B., Hubbard D.P.: Anal. Chim. Acta **35**, 85 (1966).
6. Li H., Van den Berg C.M.G.: Anal. Chim. Acta **221**, 269 (1989).
7. Israel Y., Meites L.: Encycl. Electrochem. Elem. **7**, 293 (1976).
8. Agasyan P.K., Nikoleava E.R., Khasykov V.M.: J. Anal. Chem. USSR **37**, 124 (1982)
9. Agasyan P.K., Nikolaeva E.R., Khasykov V.M.: J. Anal. Chem. USSR, **40**, 147 (1985).
10. Heumann T., Stolica N.D.: Encycl. Electrochem. Elem. **5**, 135 (1976).
11. Rigdon L.P., Harrar J.E.: Anal. Chem. **41**, 1673 (1969).
12. Miller F.J., Zittel H.E.: J. Electroanal. Chem. **7**, 116 (1964).
13. Desphande S.S., Joshi A.P.: Ind. J. Chem. **26A**, 358 (1987).
14. Wang J., Mahmoud J.S.: J. Electroanal. Chem. **208**, 383 (1986).
15. Farias P.A.M., Takase I.: Electroanalysis **4**, 823 (1992).
16. Gemmer-Colos V., Neeb R.: Naturwissenschaften **73**, 498 (1986).
17. Van den Berg C.M.G., Huang Z.Q.: Anal. Chem. **56**, 2383 (1984)
18. Adeloju S.B.O., Pablo F.: Anal. Chim. Acta **288**, 157 (1994).
19. Zhao J., Sun D., Wei X., Jin W.: Anal. Chim. Acta **306**, 225 (1995).
20. Zhou J., Neeb R.: Fres. J. Anal. Chem. **338**, 34 (1990).
21. Van den Berg C.M.G.: Anal. Chem. **57**, 1532 (1985).
22. Willie S.N., Berman S.S., Page J.A., Van Loon G.W.: Can. J. Chem. **65**, 957 (1987).
23. Quentel F., Elleouet C., Madec C.: Electroanalysis, **4**, 707 (1992).
24. Fogg A.G., Alonso R.M.: Analyst **113**, 361 (1988).
25. Wang L., Zhang X., Cheng G.: Anal. Lett. **23**, 2233 (1990).
26 Buldini P.L., Ferri D., Zignani F.: Fres. J. Anal. Chem. **314**, 660 (1983).
27. Ferri D., Buldini P.L: Analyst **107**, 1375 (1982).
28. Yokoi K., van den Berg C.M.G.: Anal. Chim. Acta **245**, 167 (1991)
29. Yamamoto Y., Hasebe K., Kambara T.: Anal. Chem. **55**, 1942 (1983).
30. Rao P.V.C., Koshy V.J.: Talanta **41**, 1911 (1994).
31. Wang J., Tian B., Lu J.: Talanta **39**, 1273 (1992).

32. Vega M., Van den Berg C.M.G.: Anal. Chim. Acta 293, 19 (1994)
33. Navrátilová Z., Kopanica M.: Anal. Chim. Acta **244**, 193 (1991).
34. Wang J., Lu J.: Talanta **39**, 801 (1992).
35. Yokoi K., Van den Berg C.M.G.: Anal. Chim. Acta, **257**, 293 (1992).
36. Kalcher K.: Electroanalysis **2**, 419 (1990).
37. Kalcher K., Kauffmann J.-M., Wang J., Švancara I., Vytřas K., Neuhold C., Yang Z.: Electroanalysis **7**, 5 (1995).
38. Specker H., Monien H., Lendermann B.: Chem. Anal. (Warsaw) **17**, 1003 (1971).
39. Monien H., Jacob P., Jänisch B.: Z. Anal. Chem. **267**, 108 (1973).
40. Monien H., Bovenkerk R., Kringe K.P., Rath D.: Fres Z. Anal. Chem. **300**, 363 (1980).
41. Stadlober M., Kalcher K., Raber G., Neuhold C.: Talanta, **43 1915** (1996).
42. Stadlober M., Kalcher K., Raber G.: Electroanalysis (1996), in press.
43. Stadlober M.
44. Kalcher K.: Fres. J. Anal. Chem. **323**, 238 (1986).
45. Kalcher K., Jorde C.: Comp. Chem. **10**, 201 (1986).
46. Starý J.: Anal. Chim. Acta **28**, 132 (1963).
47. Hu S., Yan Y., Zhao Z.: Anal. Chim. Acta **248**, 103 (1991).
48. Lin Z., Cai J.J., Scriven L.E., Davis H.T.: J. Phys. Chem. **98**, 5984 (1994).
49. Tracey A.S., Gresser M.J., Parkinson K.M.: Inorg. Chem. **26**, 629 (1987).
50. Wittick J.J., Rechnitz G.A.: Anal. Chem. **37**, 816 (1965).
51. Johansen E.S., Jons O.: Talanta **31**, 743 (1984).
52. Cruywagen J.J., Heyns J.B., Vande Water R.R.: J. Chem. Soc., Dalton Trans. 1857 (1986).